Efficient Visible-Light-Driven Photocatalysis: Simultaneous Degradation of Multiple Pollutants with Bismuth Oxyhalide Solid Solutions

Helena Pérez del Pulgar[a], Josefa Ortiz-Bustos[a], Santiago Gómez-Ruiz[a,b], Isabel del Hierro[a,b]*, Yolanda Pérez[a,c]*

[a] COMET-NANO group, Departamento de Biología y Geología, Física y Química Inorgánica, ESCET, Universidad Rey Juan Carlos, C/ Tulipán s/n, 28933 Móstoles (Madrid), Spain.

[b] Instituto de Investigación de Tecnologías para la Sostenibilidad. Universidad Rey Juan Carlos.

[c] Advanced Porous Materials Unit, IMDEA Energy, Av. Ramón de la Sagra 3, 28935 Móstoles, Madrid, Spain

E-mail: yolanda.cortes@urjc.es ; isabel.hierro@urjc.es

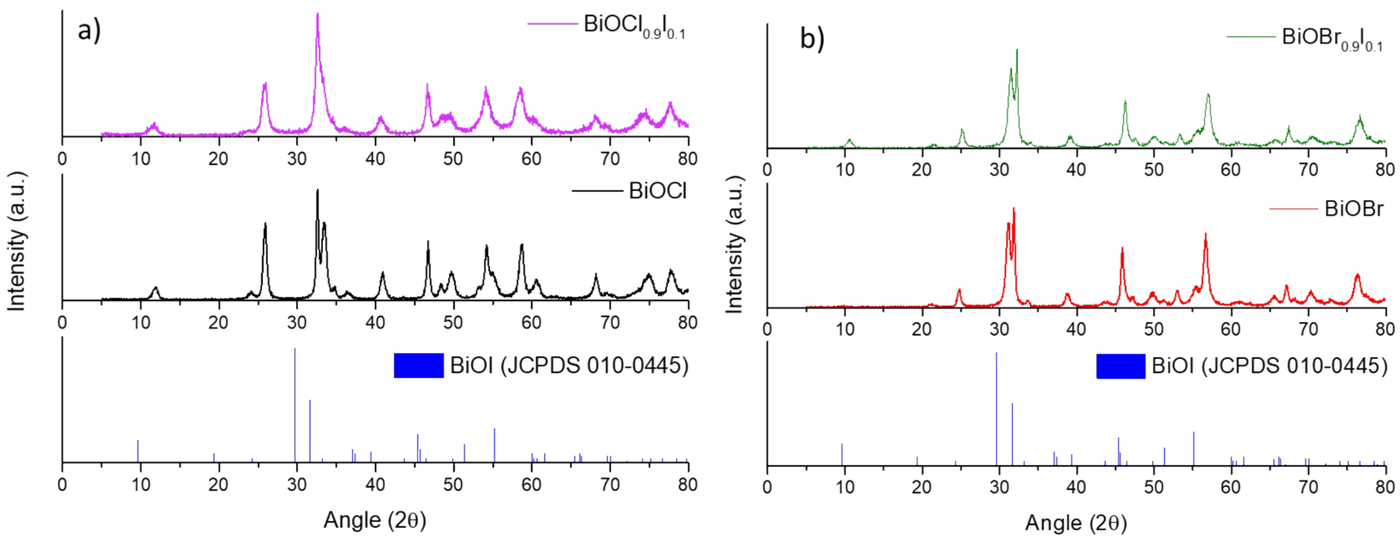

Figure S1 a) XRD spectra of $BiOCl_{0.9}I_{0.1}$ and BiOCl samples and b) XRD spectra of $BiOBr_{0.9}I_{0.1}$ and BiOBr samples, with the standard diffraction pattern of BiOI (JCPDS 010-0445).

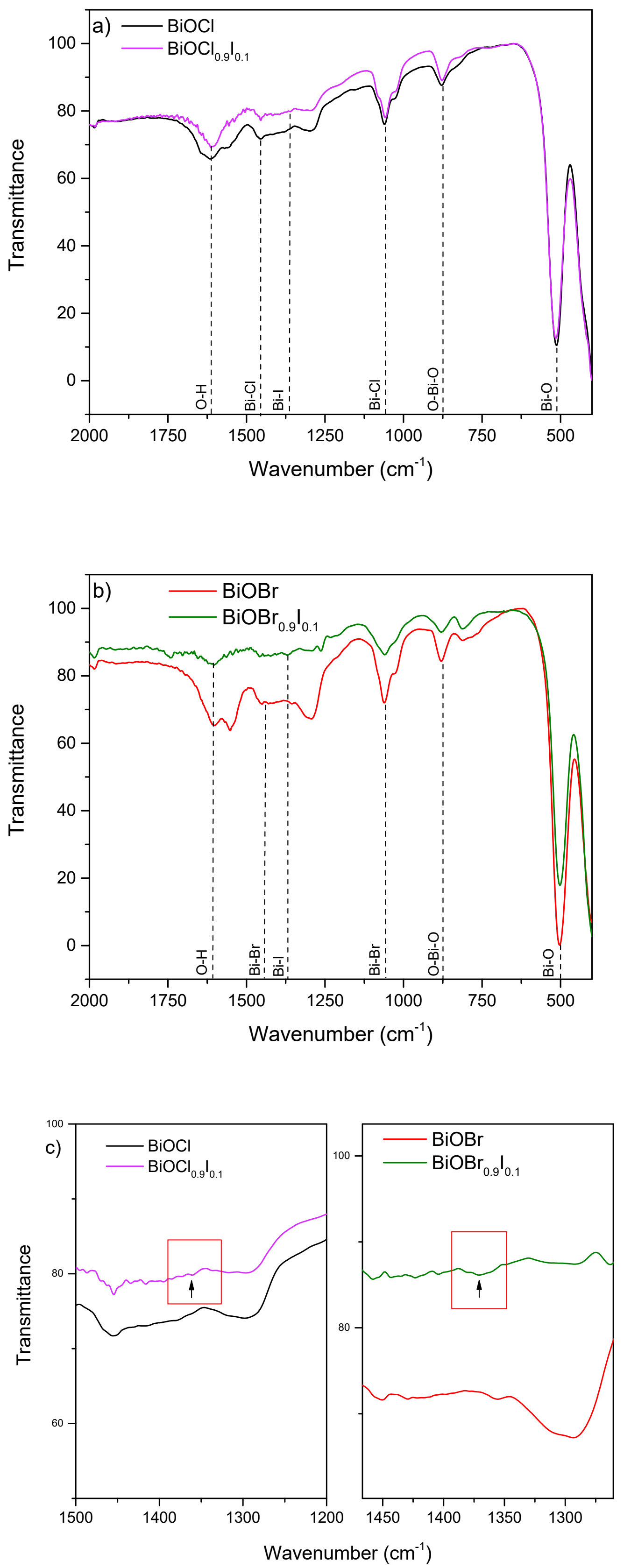

Figure S2. FT-IR spectra for a) bismuth oxychloride-based samples and b) bismuth oxybromide-based samples c) Zoom in the range 1200-1500 1366 cm^{-1}.

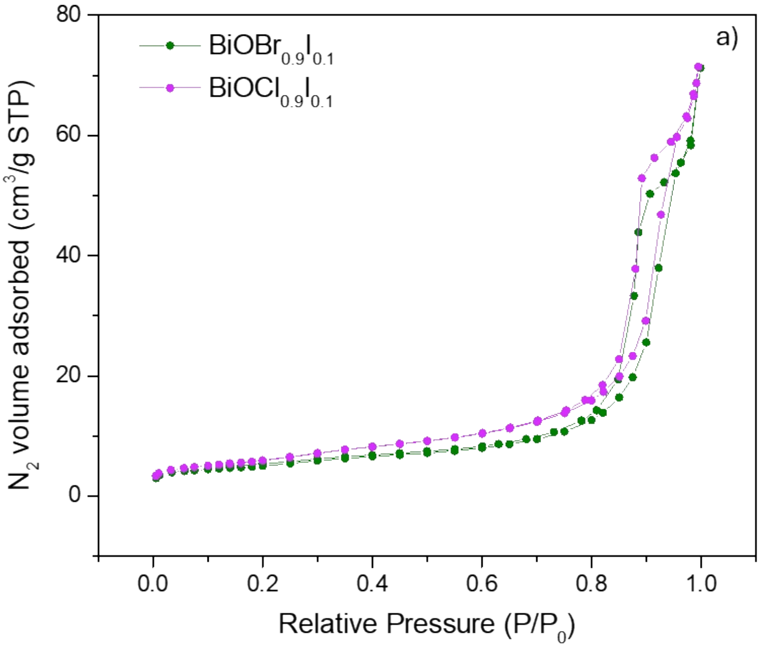

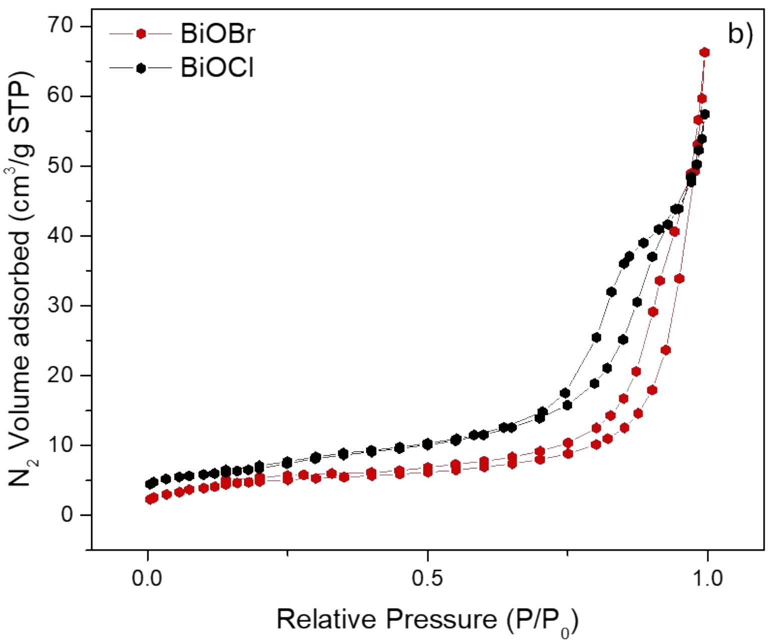

Figure S3. N_2 adsorption–desorption isotherms of the $BiOBr_{0.9}I_{0.1}$ and $BiOCl_{0.9}I_{0.1}$ samples (a) and BiOCl and BiOBr (b).

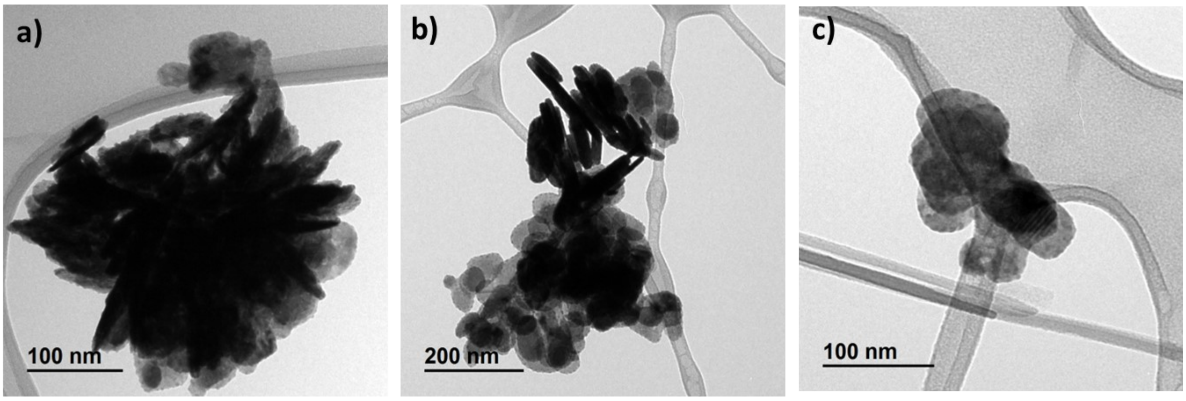

Figure S4. TEM images of $BiOCl_{0.9}I_{0.1}$ (a) and $BiOBr_{0.9}I_{0.1}$ (b) and (c)

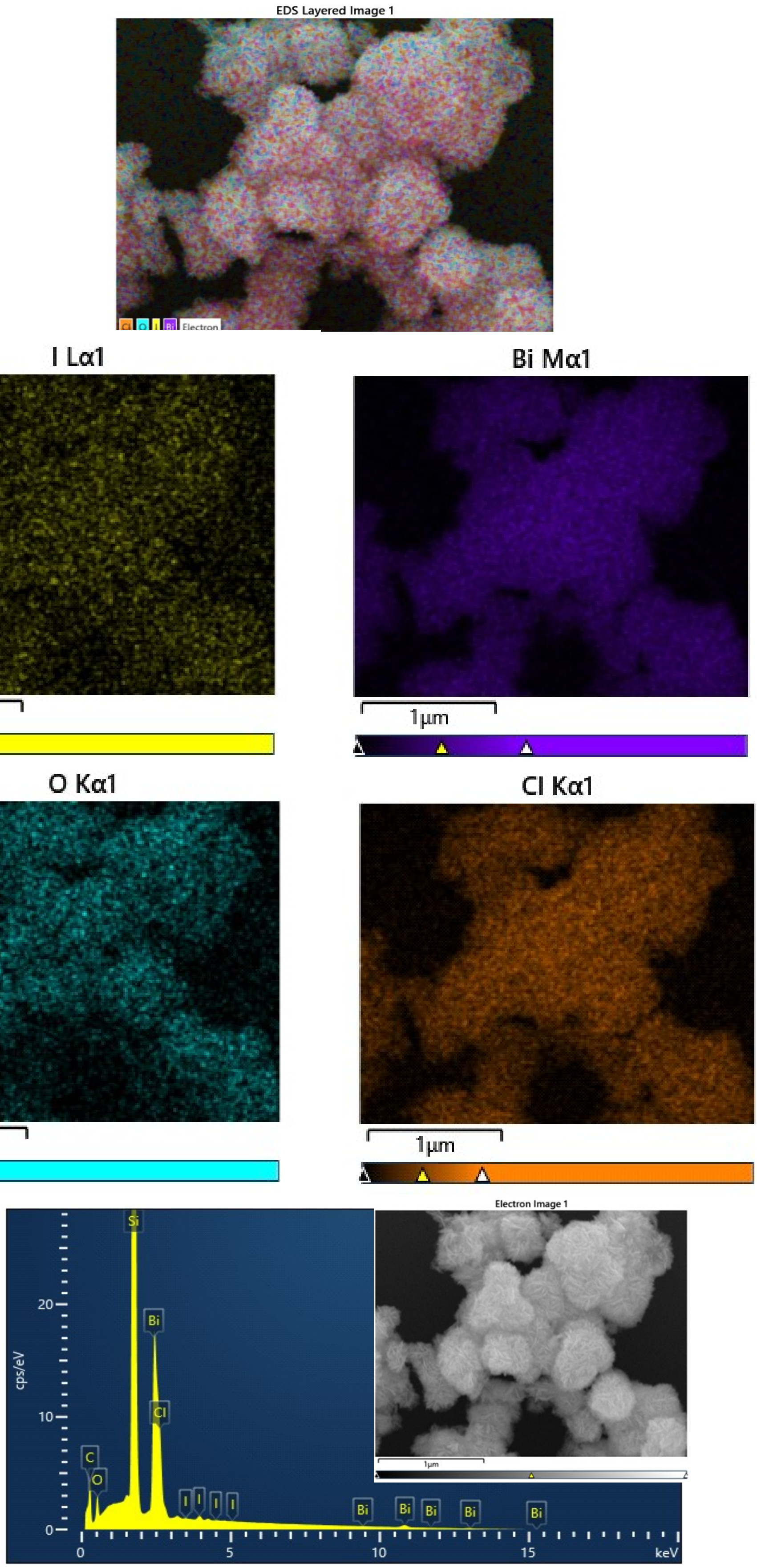

Figure S5. SEM/EDS images of the $BiOCl_{0.9}I_{0.1}$ sample. The coloured spots are the different elements in the material: yellow (I), purple (Bi), blue (O) and brown (Cl)

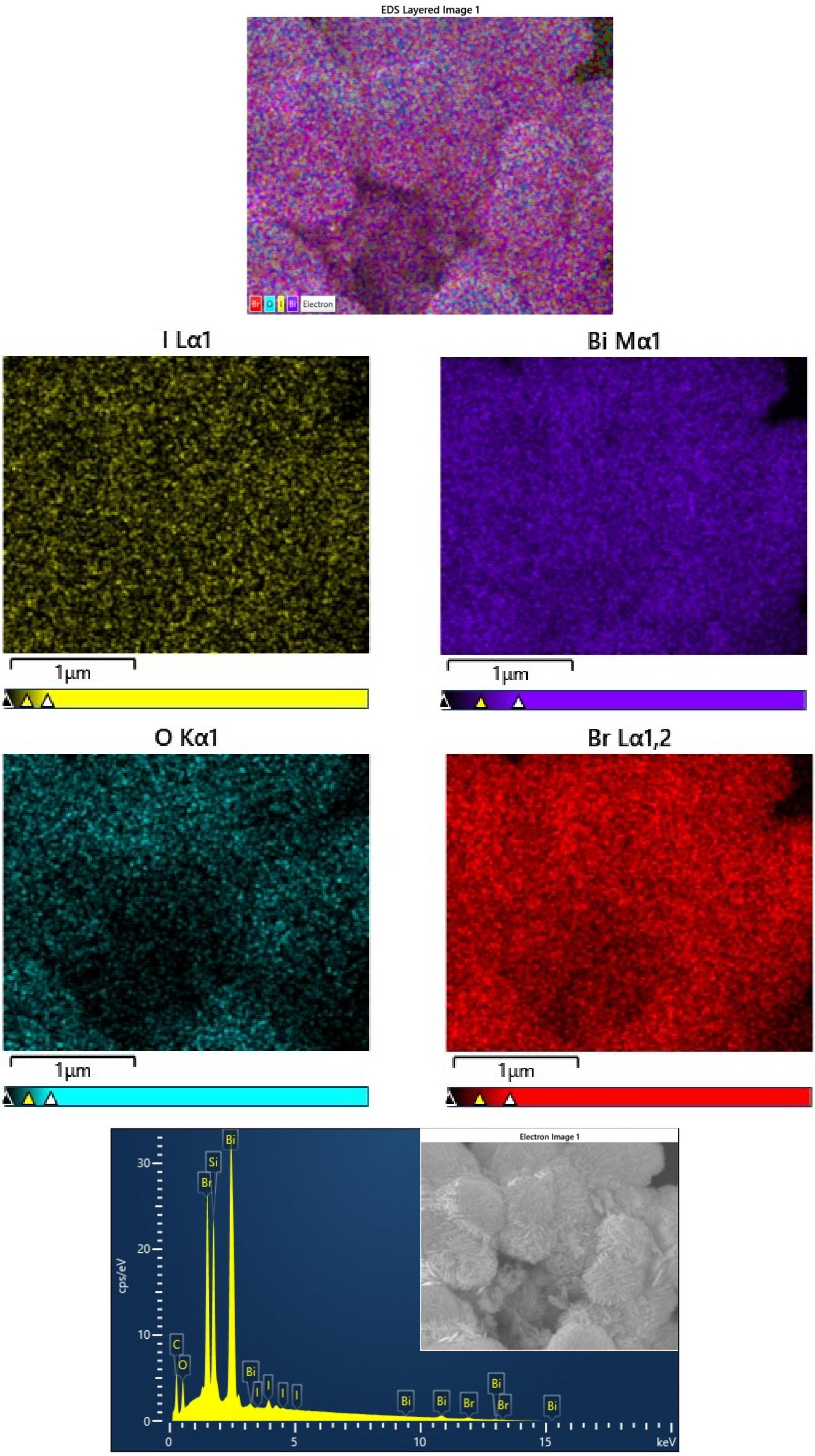

Figure S6. SEM/EDS images of the $BiOBr_{0.9}I_{0.1}$ sample. The coloured spots are the different elements in the material: yellow (I), purple (Bi), blue (O) and red (Br)

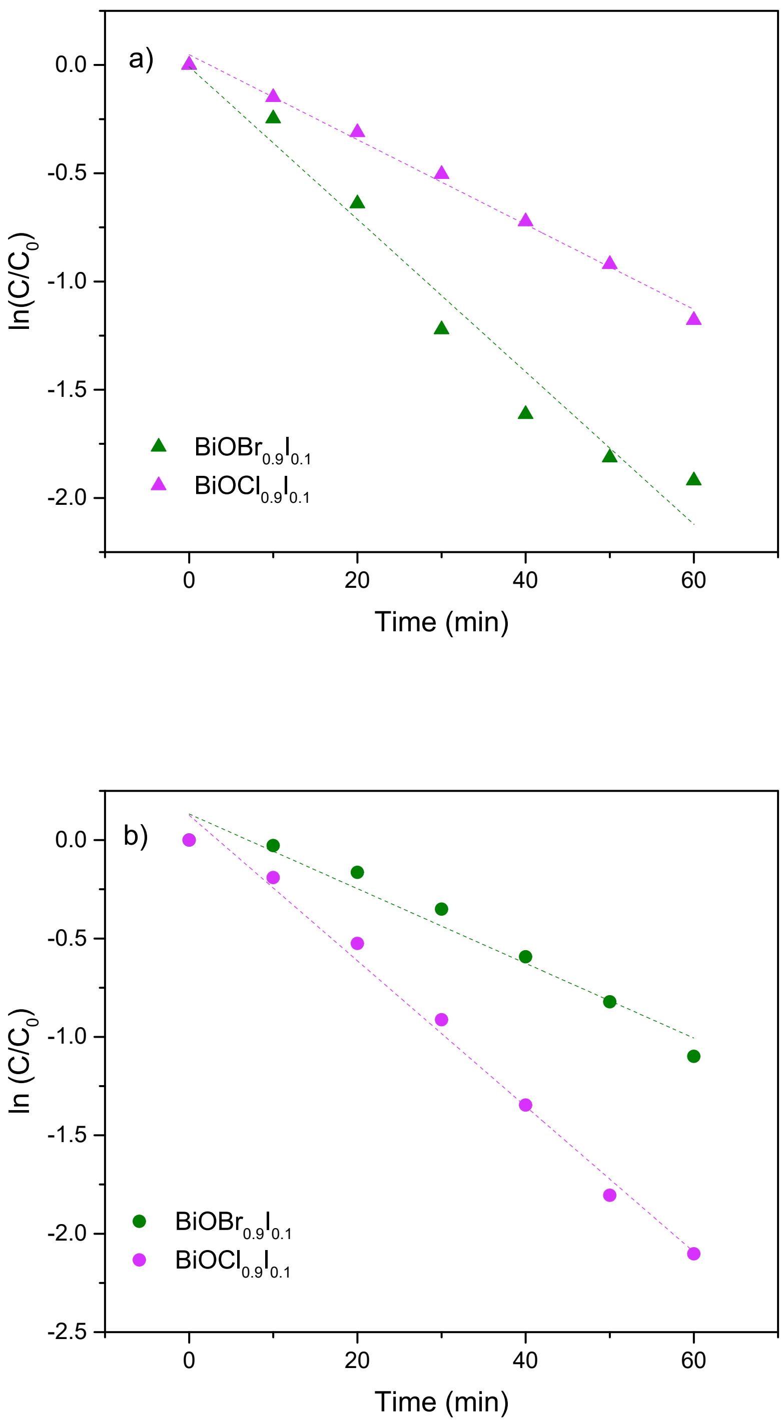

Fig. S7. Pseudo first-order kinetics of a) CIP and b) MP using bismuth oxyhalide solid solutions

Table S1. Comparison of single contaminant removal efficiencies

Photocatalyst	Contaminant	*k* (min^{-1})	C (ppm)	Removal (%)	Light source	Time (min)	Reference
$BiOCl_{0.9}I_{0.1}$	**MP**	**0.037**	**10**	**90**	**Vis (300W Xe lamp)**	**60**	**This work**
Ag/AgBr@m-WO_3	MP	0.00981	10	80	Vis (450 W Xe arc lamp)	180	1
Fe_2O_3/$BiVO_3$/biochar assembly	MP	0.020	5	95.6	Sunlight	120	2
$Bi_4O_5Br_2$	MP	0.00356	10	24.4	Vis (1000 W Xe lamp)	60	3
$I_{1.0}$-$Bi_4O_5Br_2$	MP	0.0368	10	90	Vis (1000 W Xe lamp)	60	3
$BiOBr_{0.9}I_{0.1}$	**CIP**	**0.035**	**15**	**91.6**	**Vis (300W Xe lamp)**	**60**	**This work**
3%$BiVO_4$/TiO_2	CIP	0.0215	10	100	Vis (300W Xe lamp)	120	4
BiOBr/$Bi_4O_5Br_2$	CIP	0.015	10	91	Vis (500W Xe lamp)	150	5
CuS/$BiVO_4$	CIP	0.0215	10	90	Vis (300W Xe lamp)	90	6
$BiVO_4$/Ag/MnO_2	CIP	0.0275	10	93.6	Vis (300W Xe lamp)	100	7
Ag-$BiVO_4$	CIP	0.02814	10	98.2	Solar light	120	8

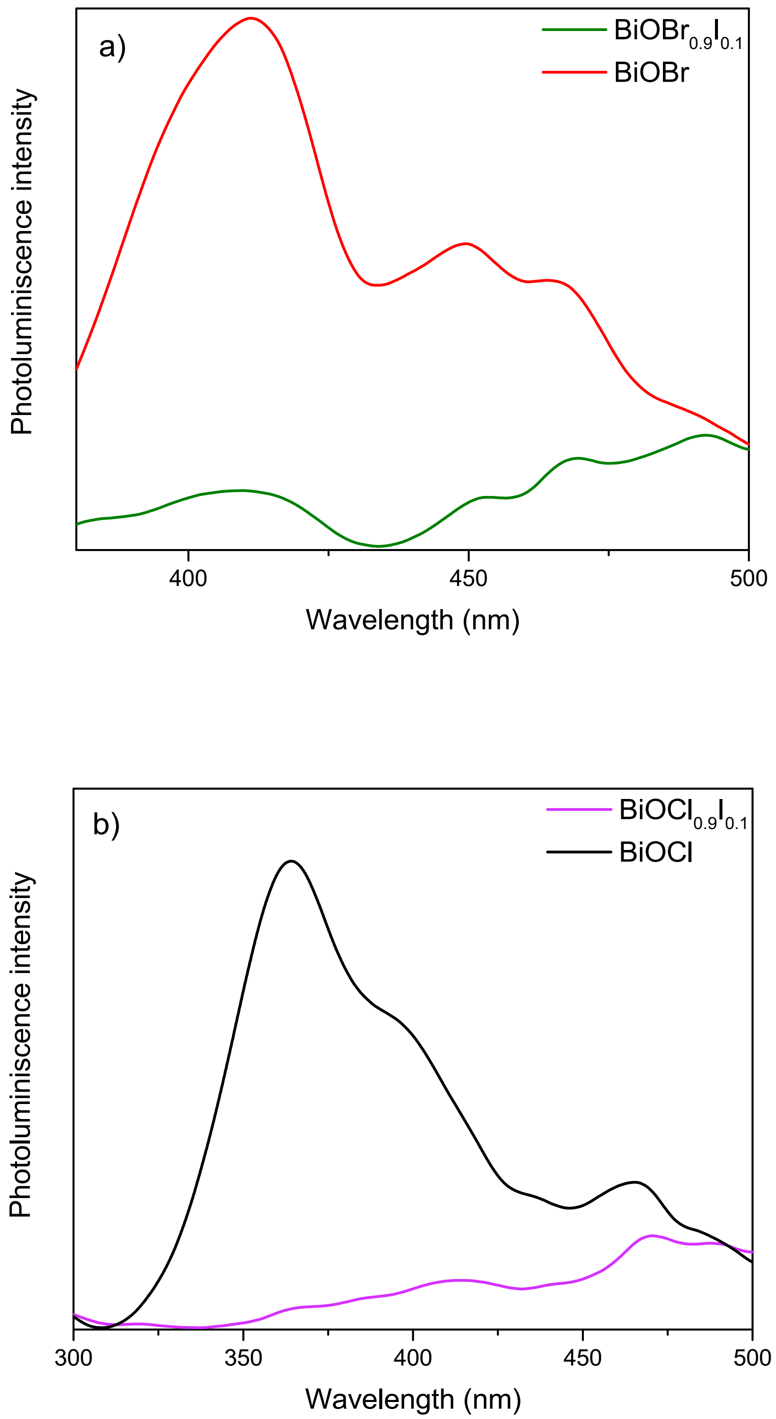

Figure S8. PL spectra of a) BiOBr-based samples upon excitation at 315 nm (cut wavelength 370 nm) and b) BiOCl-based samples upon excitation at 266 nm (cut wavelength 290 nm)

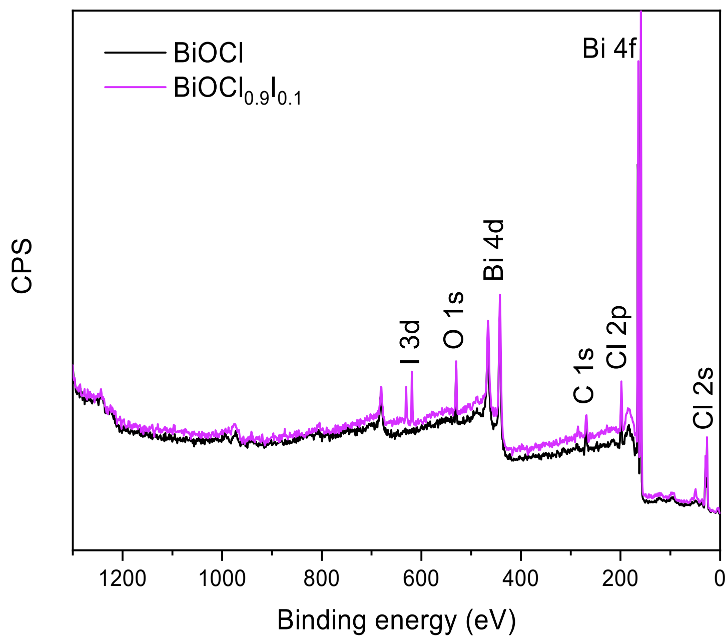

Figure S9. XPS survey spectra of bismuth oxychloride-based samples

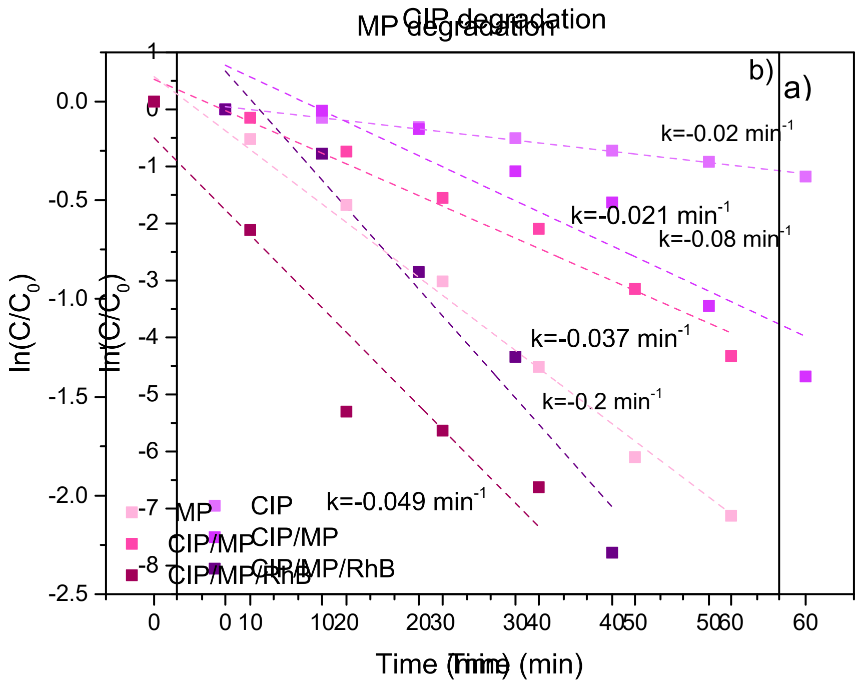

CIP degradation
MP degradation
a)
b)
ln(C/C0)
Time (min)
k=-0.02 min-1
k=-0.021 min-1
k=-0.08 min-1
k=-0.037 min-1
k=-0.2 min-1
k=-0.049 min-1
MP
CIP/MP
CIP/MP/RhB
CIP
CIP/MP
CIP/MP/RhB

Figure S10. Pseudo first-order kinetics of a) CIP and b) MP degradation using $BiOCl_{0.9}I_{0.1}$ in a single-, binary- (CIP/MP) and ternary-contaminant system (CIP/MP/RhB).

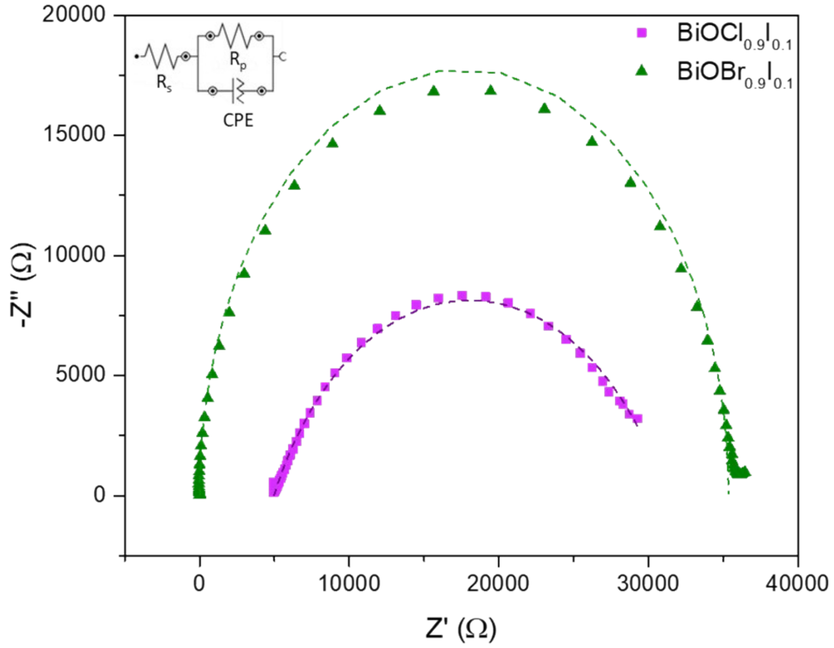

Figure S11. Electrochemical impedance measurements, Nyquist plots of $BiOX_{0.9}I_{0.1}$ carbon paste electrodes

Table S2. Values obtained by the Randles model circuit fitting of EIS spectra of $BiOX_{0.9}I_{0.1}$.

Material	R_S (kΩ)	R_p (kΩ)	CPE (μMho*s^N)
$BiOCl_{0.9}I_{0.1}$	4.89	26.2	6.86
$BiOBr_{0.9}I_{0.1}$	27.0	35.3	96.4

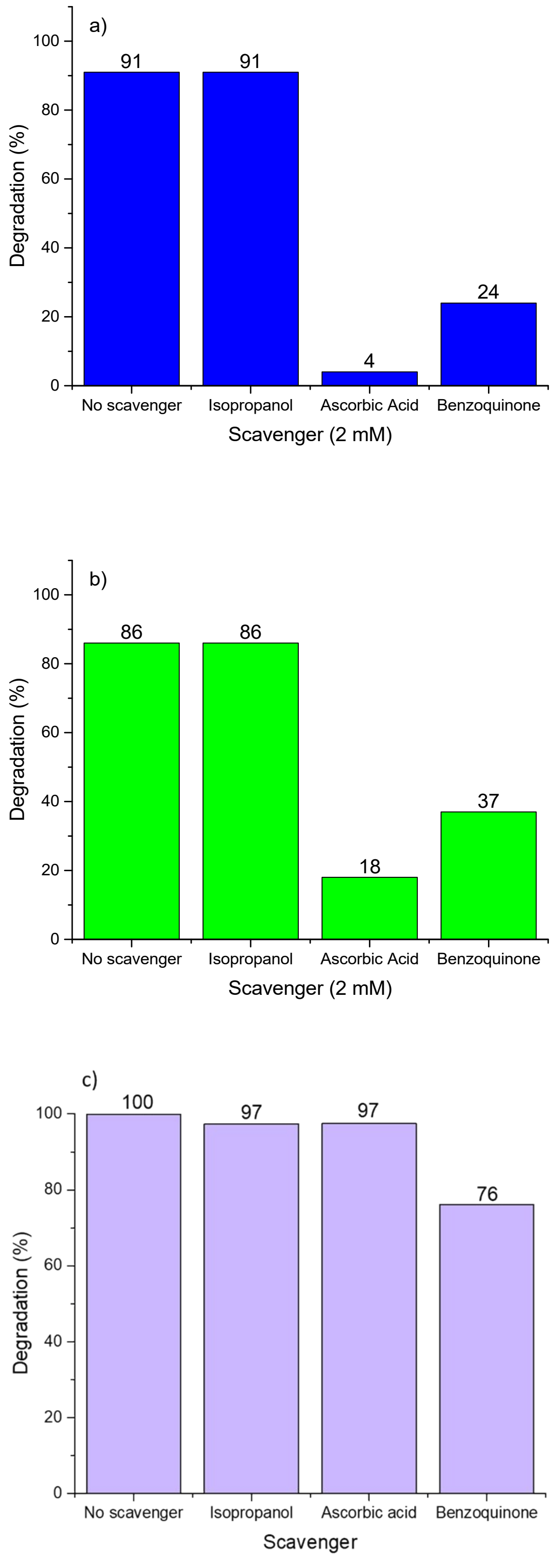

Fig. S12. Scavenger experiments for MP degradation using $BiOCl_{0.9}I_{0.1}$ a) single-contaminant (final time = 80 min) and b) ternary-contaminant system (final time = 40 min). c) Scavenger experiments for CIP degradation using $BiOCl_{0.9}I_{0.1}$ in the ternary-contaminant system (final time = 40 min).

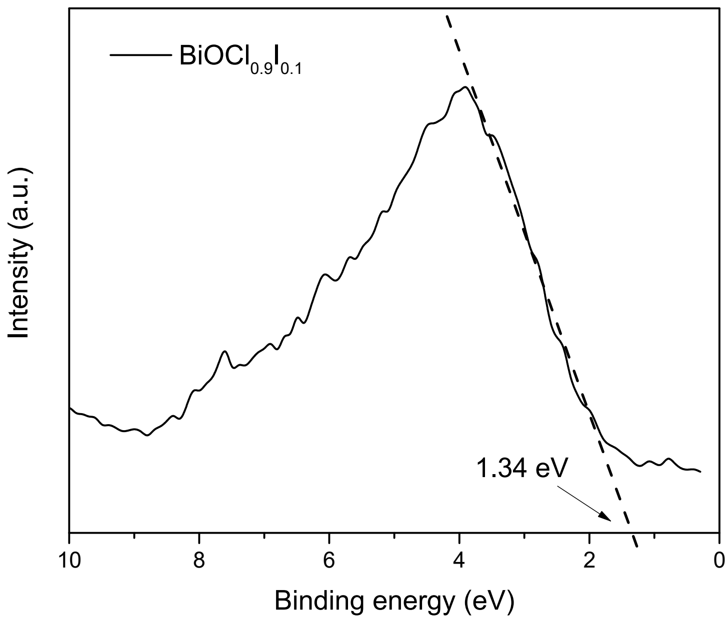

Fig. S13. XPS spectrum of the valence band potential ($E_{VB\text{-}XPS}$) for $BiOCl_{0.9}I_{0.1}$

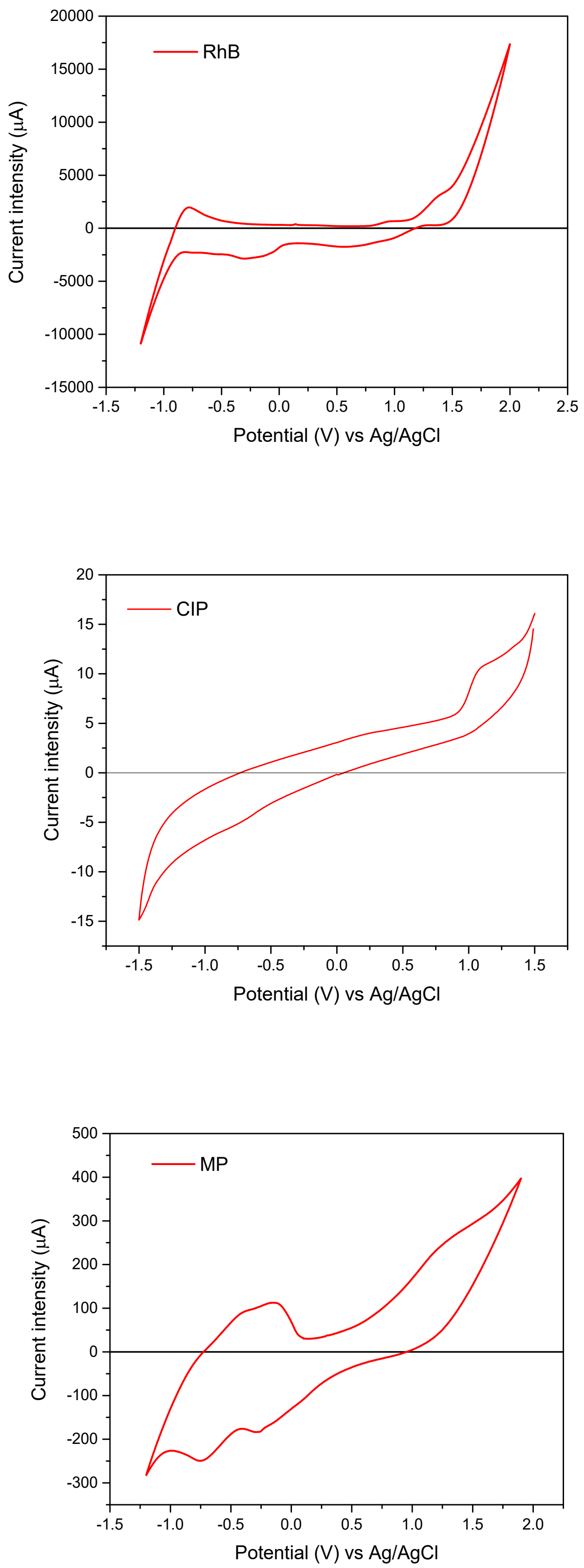

Fig. S14. CV of RhB, CIP and MP in PBS at pH 7.4 using Pt as both the working and counter electrodes and Ag/AgCl/KCl 3M as a reference electrode.

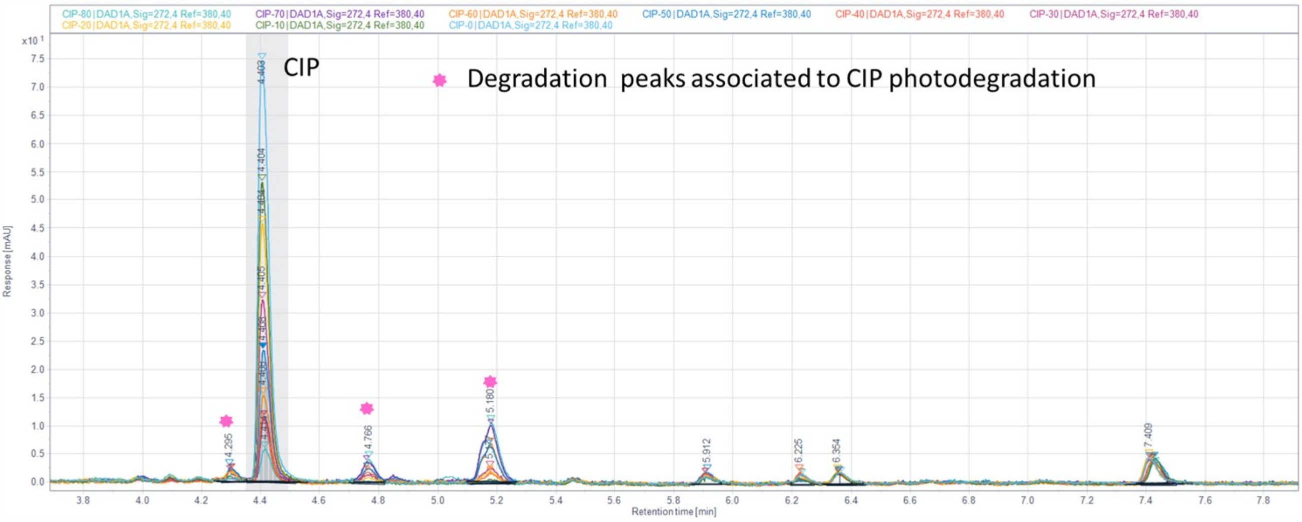

Figure S15. HPLC chromatogram of the CIP degradation in the single system at 272 nm using $BiOCl_{0.9}I_{0.1}$.

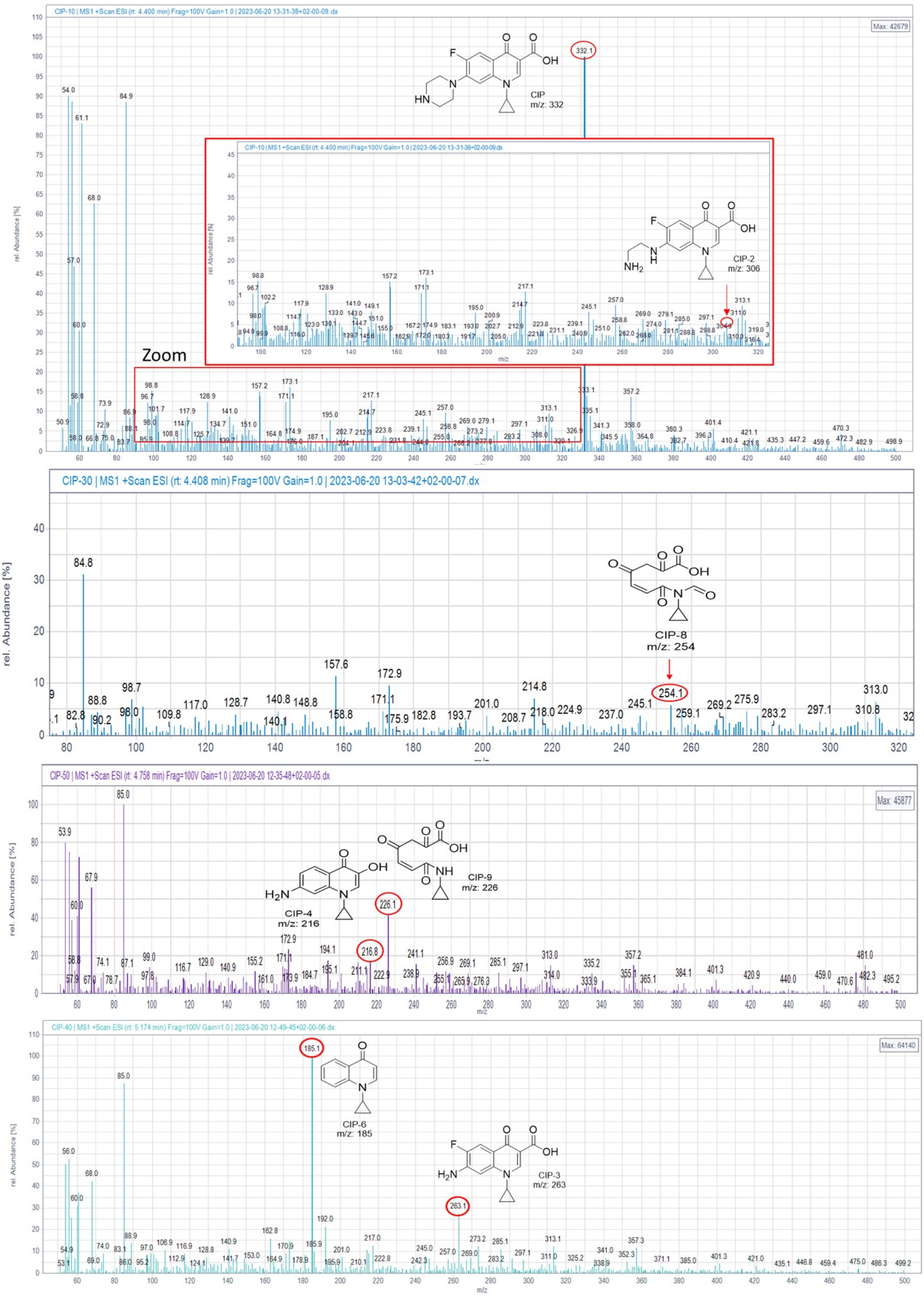

Fig. S16. LC-MS spectra of the CIP degradation in the single system using $BiOCl_{0.9}I_{0.1}$.

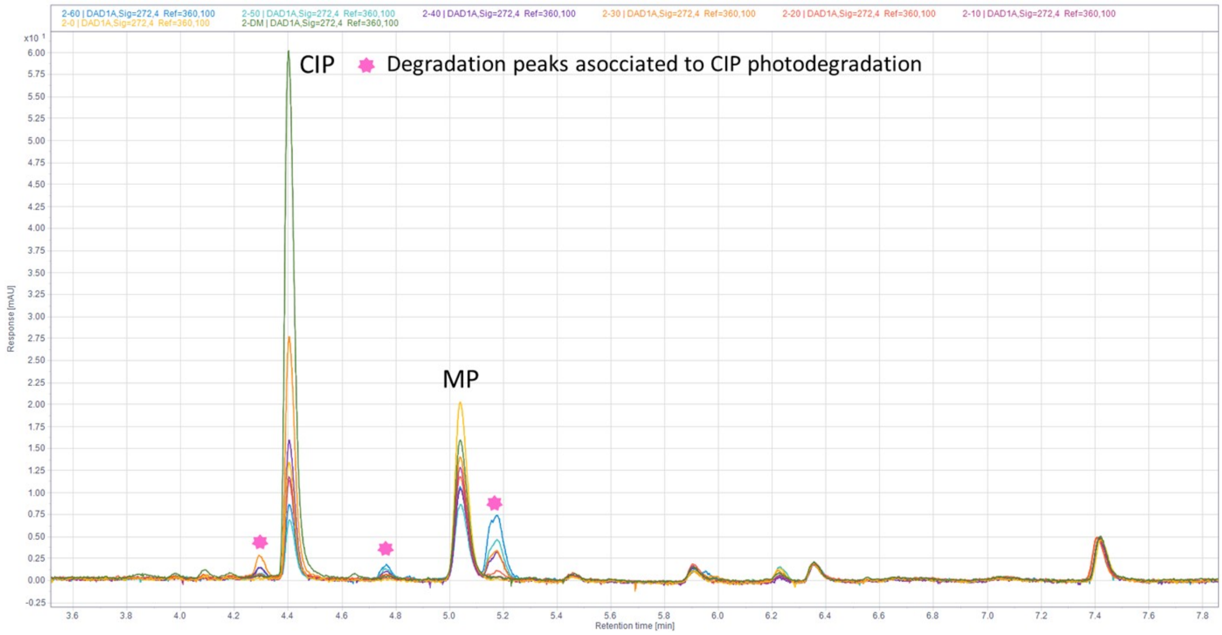

Fig. S17. HPLC chromatogram of the CIP degradation in the binary-contaminant system (CIP/MP) at 272 nm using $BiOCl_{0.9}I_{0.1}$.

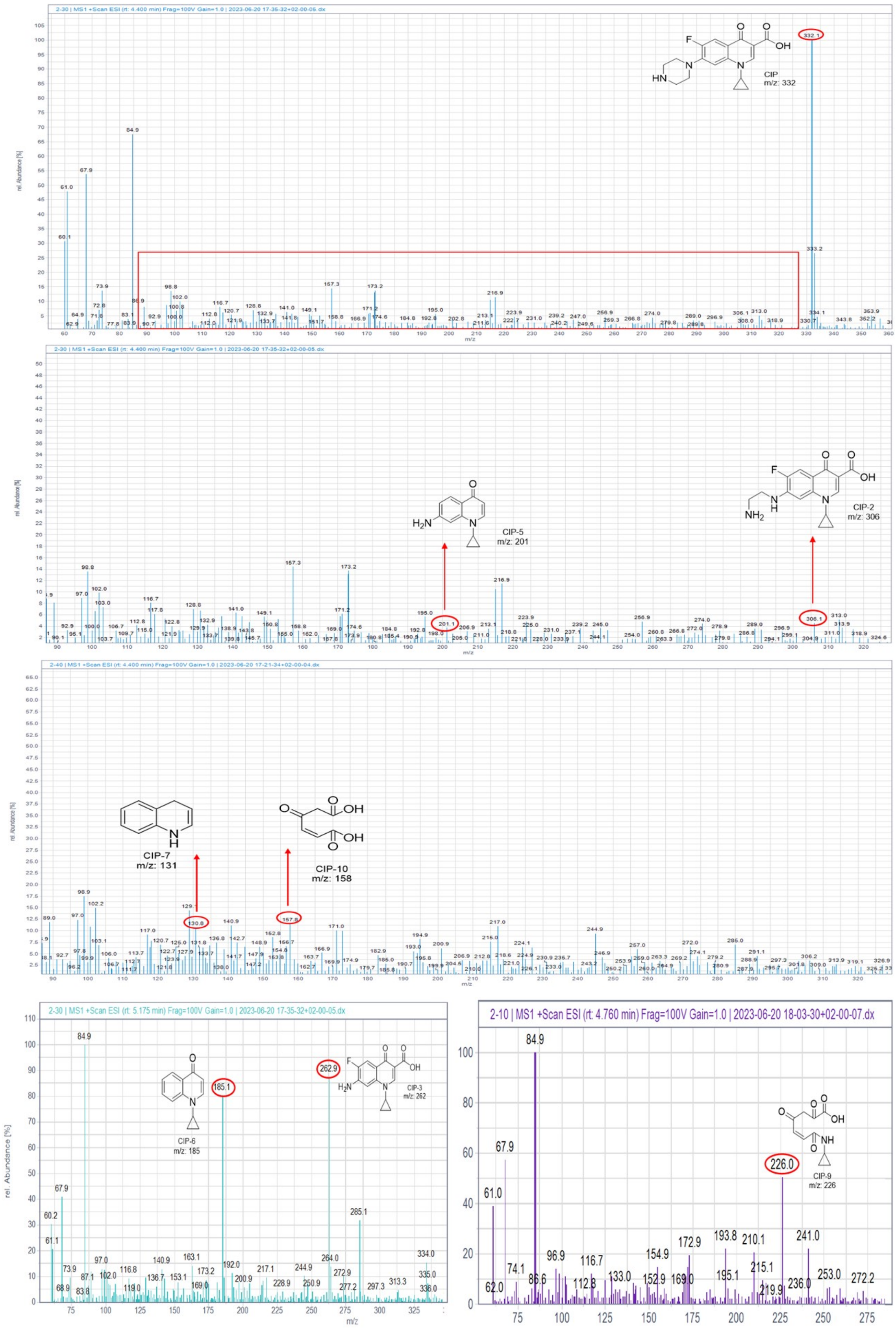

Fig. S18. LC-MS spectra of the CIP degradation in the binary-contaminant system (CIP/MP) using $BiOCl_{0.9}I_{0.1}$

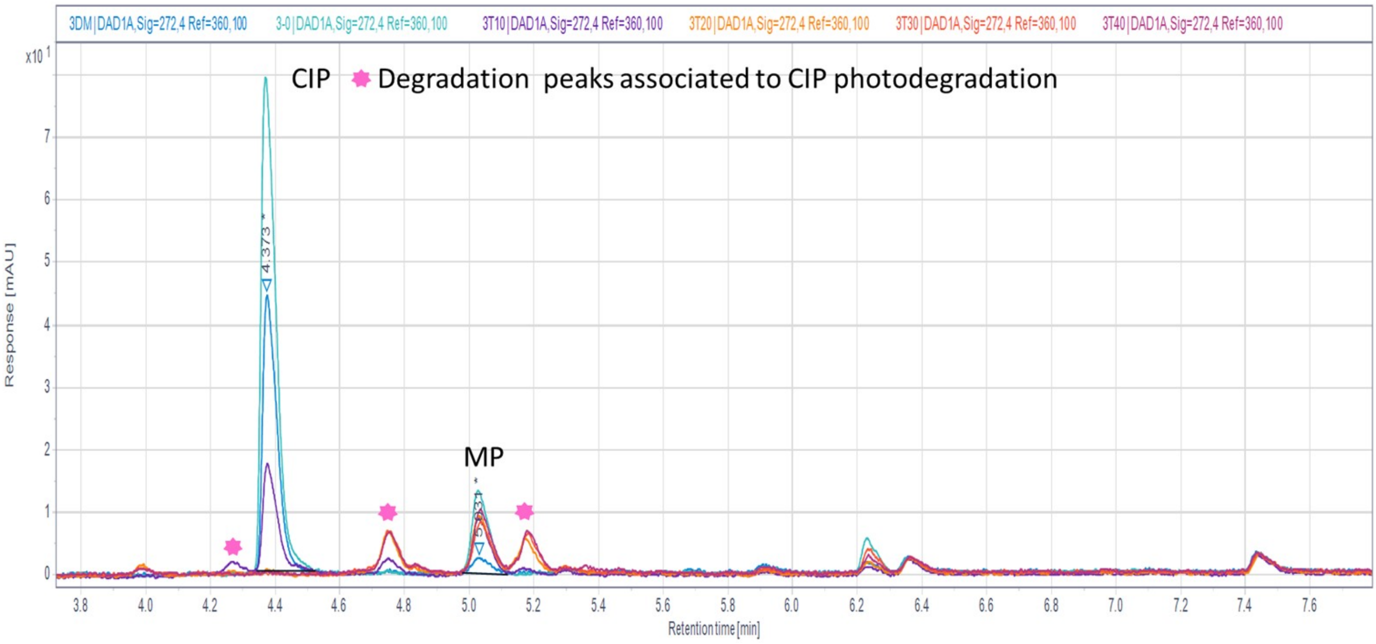

Fig. S19. HPLC chromatogram of the CIP degradation in the ternary-contaminant system (CIP/MP/RhB) at 272 nm using $BiOCl_{0.9}I_{0.1}$.

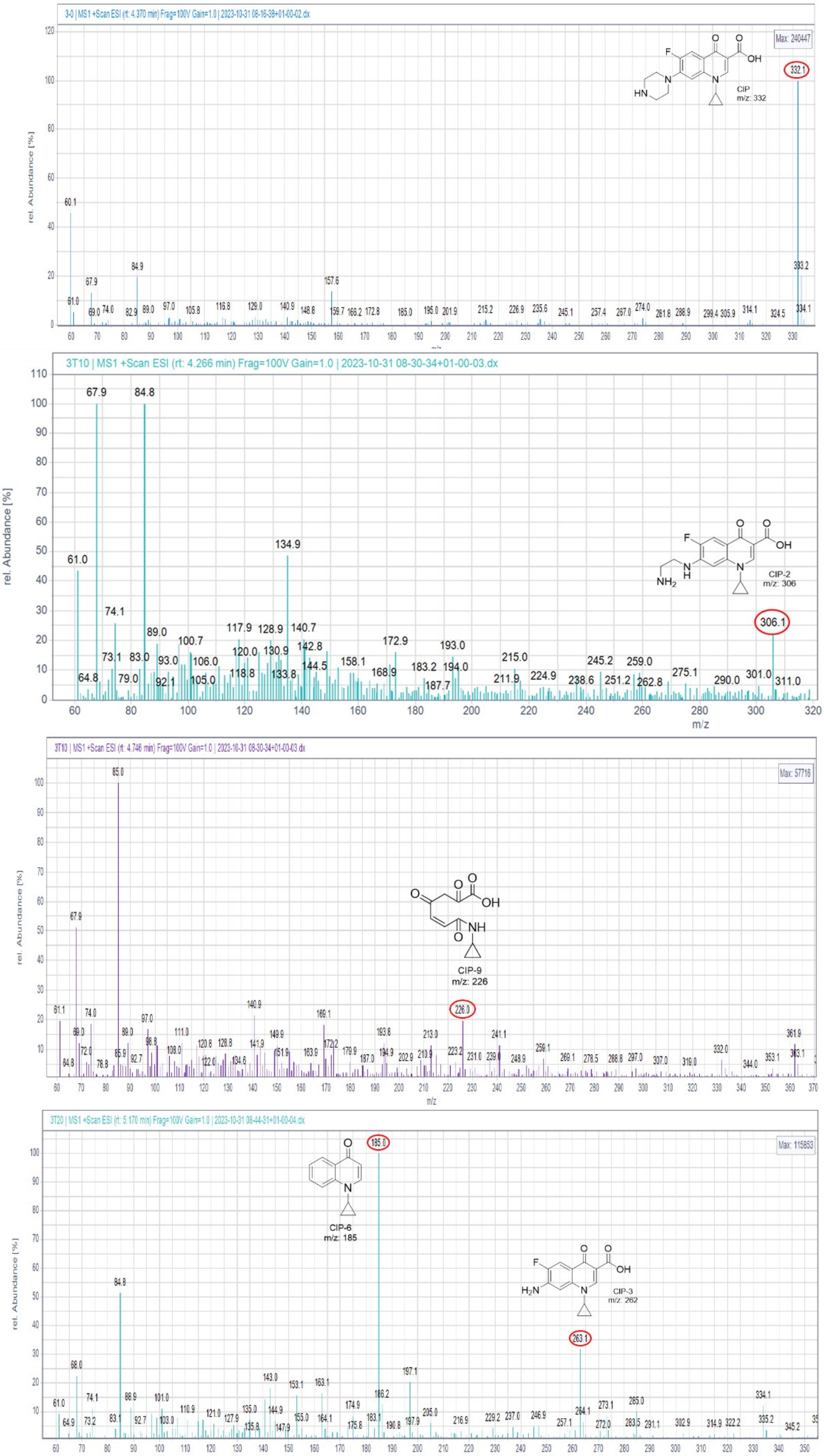

Fig. S20. LC-MS spectra of the CIP photodegradation in the ternary-contaminant system (CIP/MP/RhB) using $BiOCl_{0.9}I_{0.1}$.

Table S3. Predicted toxicity of the CIP molecule and their degradation intermediates

Molecules	MS/MZ values	Molecular formula	Fish (LC_{50}) (mg/L)		Daphnid (LC_{50}) (mg/L)	
			Predicted toxicity	Toxic/non-toxic*	Predicted toxicity	Toxic/non-toxic*
CIP	331	$C_{17}H_{18}FN_3O_3$	0.2	Very toxic	N/A	---
CIP-2	305	$C_{15}H_{16}FN_3O_3$	0.1	Very toxic	11.98	Harmful
CIP-3	262	$C_{13}H_{11}FN_2O_3$	0.2	Very toxic	23.5	Harmful
CIP-4	216	$C_{12}H_{12}N_2O_2$	2.9	Toxic	21.75	Harmful
CIP-5	200	$C_{12}H_{12}N_2O$	0.4	Very toxic	8.38	Toxic
CIP-6	185	$C_{12}H_{11}NO$	2.5	Toxic	4.17	Toxic
CIP-7	131	C_9H_9N	24.3	Harmful	95.75	Harmful
CIP-8	253	$C_{11}H_{11}NO_6$	36.11	Harmful	472.94	Not harmful
CIP-9	225	$C_{10}H_{11}NO5$	45.72	Harmful	568.53	Not harmful
CIP-10	158	$C_6H_6O_5$	118.95	Not harmful	433.57	Not harmful

* Standard toxicity range – Very Toxic - $LC_{50} < 1$; Toxic – $1 < LC_{50} < 10$; Harmful – $10 < LC_{50} < 100$; Not Harmful $LC_{50} > 100$.

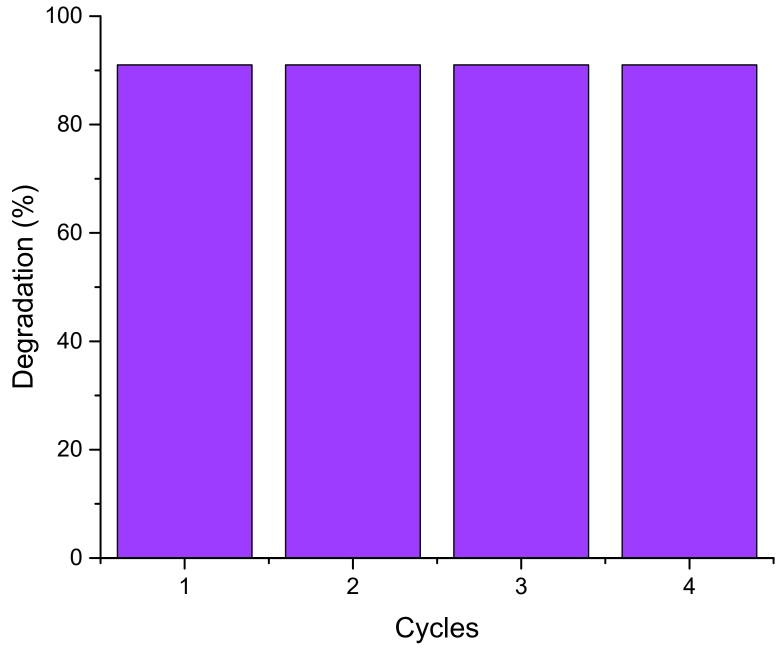

Figure S21. Recycling of $BiOCl_{0.9}I_{0.1}$ for MP degradation.

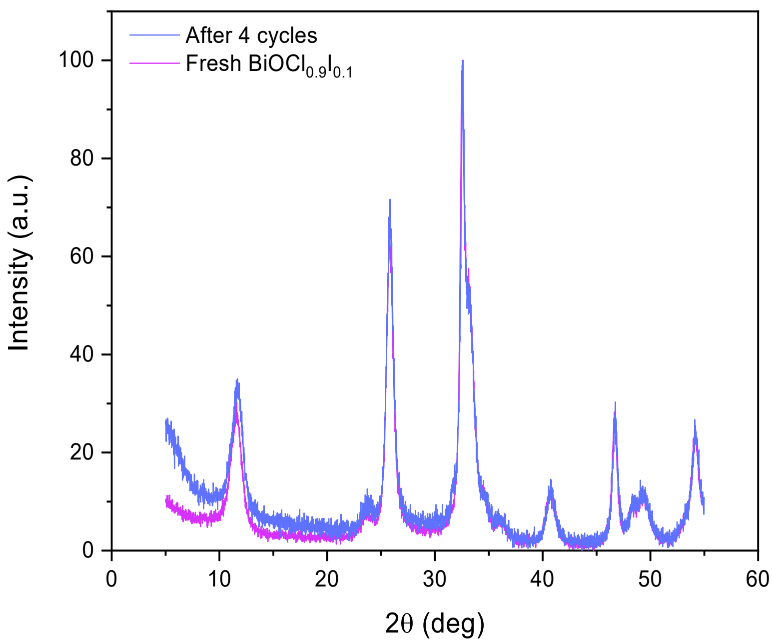

Fig S22. PXRD patters of fresh $BiOCl_{0.9}I_{0.1}$ material and after 4 cycles of MP photodegradation

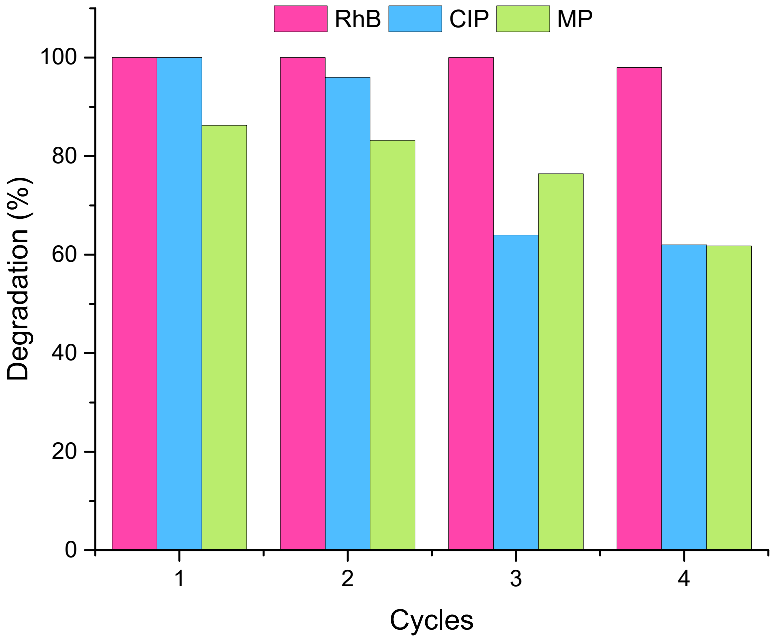

Figure S23. Recycling of $BiOCl_{0.9}I_{0.1}$ in the ternary-contaminant system (CIP/MP/RhB) (final time = 40 min)

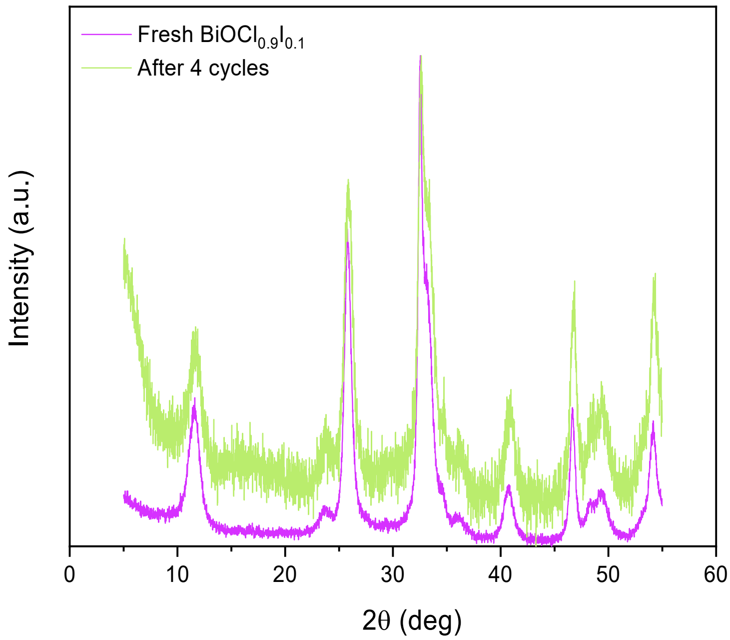

Fig S24. PXRD patters of $BiOCl_{0.9}I_{0.1}$ before and after 4 cycles in the ternary-contaminant system (CIP/MP/RhB).

References

1. Suliman, M. A.; Gondal, M. A.; Dastageer, M. A.; Chuah, G.; Basheer, C., *Photochem. Photobiol.* 2019, **95**, 1485-1494.

2. Kumar, A.; Shalini; Sharma, G.; Naushad, M.; Kumar, A.; Kalia, S.; Guo, C.; Mola, G. T., *J. Photochem. Photobiol. A.* 2017, **337**, 118-131.

3. Xiao, X.; Lu, M.; Nan, J.; Zuo, X.; Zhang, W.; Liu, S.; Wang, S., *Appl. Catal., B,* 2017, **218**, 398-408.

4. Tashkandi, N. Y.; Albukhari, S. M.; Ismail, A. A., *Environ. Sci. Pollut. Res.* 2022, **29,** 78472-78482.

5. Su, X.; Wu, D., *Mat. Sci. Semicond. Process.* 2018, **80**, 123-130.

6. Lai, C.; Zhang, M.; Li, B.; Huang, D.; Zeng, G.; Qin, L.; Liu, X.; Yi, H.; Cheng, M.; Li, L.; Chen, Z.; Chen, L., *Chem. Eng. J.* 2019, **358**, 891-902.

7. Qin, T.; Wei, J.; Zhou, C.; Zeng, X.; Zhou, J.; Li, Y., *Sep. Purif. Technol.* 2023, **317**, 123793.

8. Abid, M. Z.; Ilyas, A.; Rafiq, K.; Rauf, A.; Nadeem, M. A.; Waseem, A.; Hussain, E., *Environ. Sci. Water. Res. Technol.* 2023, **9,** 2238-2252.